

# A multi-photon magneto-optical trap

Saijun Wu, Thomas Plisson, Roger Brown, William D. Phillips and J. V. Porto

*Joint Quantum Institute, NIST and University of Maryland, Gaithersburg, Maryland 20899*

(Dated: September 10, 2009)

## Abstract

We demonstrate a Magneto-Optical Trap (MOT) configuration which employs optical forces due to light scattering between electronically excited states of the atom. With the standard MOT laser beams propagating along the  $x$ - and  $y$ - directions, the laser beams along the  $z$ -direction are at a different wavelength that couples two sets of *excited* states. We demonstrate efficient cooling and trapping of cesium atoms in a vapor cell and sub-Doppler cooling on both the red and blue sides of the two-photon resonance. The technique demonstrated in this work may have applications in background-free detection of trapped atoms, and in assisting laser-cooling and trapping of certain atomic species that require cooling lasers at inconvenient wavelengths.

PACS numbers: 37.10.De, 37.10.Vz, 32.80.Wr

The development of laser cooling and trapping techniques in the last three decades has greatly enhanced our ability to control atoms, impacting a range of fields from precision atomic measurements and atomic clocks to quantum degenerate gases and quantum information processing. To date, most laser cooling methods use the mechanical effect of single-photon transitions between ground states and electronically excited states. These include Doppler cooling, polarization gradient cooling, and velocity-selective coherent population trapping [1]. There are, however, a few theoretical and experimental studies involving laser cooling in three-level systems comprising a ground state and two electronically excited states. For example, ref. [2] showed an enhancement of radiation pressure by driving a 2-photon transition in a 3-level system. In other work, the effective linewidth for the cooling transition was controlled by dressing the excited state via a coupling to another excited state. This effect can either broaden [3, 4] or narrow [5] the effective single-photon cooling transition.

Exploiting the Doppler and Zeeman shifts of single-photon optical dipole transitions, the Magneto-Optical Trap (MOT) [6] has been the standard tool to cool and trap neutral atoms in 3D. The primary motivation of this work is to use Doppler and Zeeman shifts of multi-photon transitions to both cool and trap atoms. We demonstrate a trap geometry where the cooling and trapping of atoms along one axis of the 3D-trap is due entirely to optical forces from transitions between two *electronically excited* states [7]. Specifically, with the 852 nm cooling laser beams of a standard cesium( $^{133}\text{Cs}$ ) MOT propagating along the  $x$ - and  $y$ - directions, we replace the laser beams along the  $z$ -direction with counter-propagating 795 nm laser beams that only couple the excited states of cesium ( $6\text{P}_{3/2} F'=5$ ) to a third set of excited states ( $8\text{S}_{1/2} F''=4$ ) (see Fig. 1). In this two-color MOT we find efficient cooling along the  $z$ -direction at both small and large two-photon detunings, while a magneto-optical restoring force was found when the helicities of the 6P-8S beams are opposite to those for the standard MOT. Remarkably, the two-color MOT can reach sub-Doppler temperatures at both positive and negative two-photon detunings.

The new feature of the two-color MOT sketched in Fig. 1 is in the cooling and trapping along the  $z$ - direction. Consider the low intensity regime where the rate of excited atoms leaving from both  $6\text{P}_{3/2}$  and  $8\text{S}_{1/2}$  states is dominated by spontaneous emission, with negligible contribution from stimulated processes. In this regime, the dominant radiation pressure along  $\hat{\mathbf{z}}$  is due to 2-photon scattering, where the first photon is absorbed from the

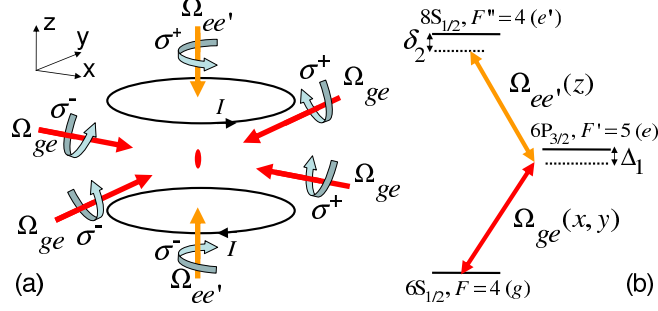


FIG. 1: (Color online) (a): Schematic of the setup in this work;  $\sigma^\pm$  are specified with respect to the positive  $x$ ,  $y$  and  $z$  axes. (b): Simplified level diagram and related transitions.

in-plane laser beams and the second is absorbed from the beams along  $\hat{\mathbf{z}}$ . In particular, we consider  $R_{\hat{\mathbf{i}}\hat{\mathbf{j}}}^{(2)}$ , the rate of 2-photon scattering induced by a 6S-6P beam along  $\hat{\mathbf{i}}$  and a 6P-8S beam along  $\hat{\mathbf{j}}$ . Here  $\hat{\mathbf{i}} \in \{\hat{\mathbf{x}}, -\hat{\mathbf{x}}, \hat{\mathbf{y}}, -\hat{\mathbf{y}}\}$  is one of the four directions of the 6S-6P beams, and  $\hat{\mathbf{j}} \in \{\hat{\mathbf{z}}, -\hat{\mathbf{z}}\}$  is one of the two directions of the 6P-8S beams. The scattering force along  $\hat{\mathbf{z}}$  can be written as  $\mathbf{f}_z^{(2)} = \hbar k_{ee'} \sum_{\hat{\mathbf{i}}\hat{\mathbf{j}}} R_{\hat{\mathbf{i}}\hat{\mathbf{j}}}^{(2)} \hat{\mathbf{j}}$ . For an atom moving at velocity  $\mathbf{v}$ , we have the 2-photon scattering rate in the low intensity limit:

$$R_{\hat{\mathbf{i}}\hat{\mathbf{j}}}^{(2)} = \frac{\gamma |\Omega_{ge} \Omega_{ee'}|^2}{16 |(\tilde{\Delta}_1 - k_{ge} \hat{\mathbf{i}} \cdot \mathbf{v})(\tilde{\delta}_2 - k_{ge} \hat{\mathbf{i}} \cdot \mathbf{v} - k_{ee'} \hat{\mathbf{j}} \cdot \mathbf{v})|^2}. \quad (1)$$

Here  $\Omega_{ge}$  and  $\Omega_{ee'}$  are the Rabi frequencies of the laser induced couplings per beam;  $k_{ge}$  and  $k_{ee'}$  are the wavenumbers of the laser beams;  $\tilde{\Delta}_1 = \Delta_1 + i\Gamma/2$  and  $\tilde{\delta}_2 = \delta_2 + i\gamma/2$ ;  $\Delta_1$  and  $\delta_2$  are the 1-photon and 2-photon detunings for the  $6S_{1/2} F=4$  to  $8S_{1/2} F''=4$  2-photon excitation, with  $6P_{3/2} F'=5$  as the intermediate level (Fig. 1b);  $\Gamma/2\pi = 5.2$  MHz and  $\gamma/2\pi = 1.5$  MHz are the linewidths of the  $6P_{3/2}$  and  $8S_{1/2}$  states respectively.

Taylor-expanding Eq. (1) around  $v_z = \hat{\mathbf{z}} \cdot \mathbf{v} = 0$  gives  $f_z^{(2)} \approx -\alpha^{(2)} v_z$ , with  $\alpha^{(2)} > 0$  (damping) for negative 2-photon detuning  $\delta_2 < 0$ . This 2-photon version of the usual [1] Doppler cooling mechanism can be summarized with the level diagram in Fig. 2a: the Doppler effect enhances the absorption cross-section for the 6P-8S beam opposing the velocity. One qualitative difference from standard Doppler cooling is that the 2-photon transitions to the 8S states are not closed, so we expect that repumping light will be important to keep the population from pumping into the  $6S_{1/2} F=3$  ground states.

In addition to the velocity-dependent force, a position-dependent restoring force along the  $z$ -direction is essential for trapping. Figure. 2b illustrates the basic principle of the trapping force. To simplify our discussion, we consider a hypothetical atom with angular momentum

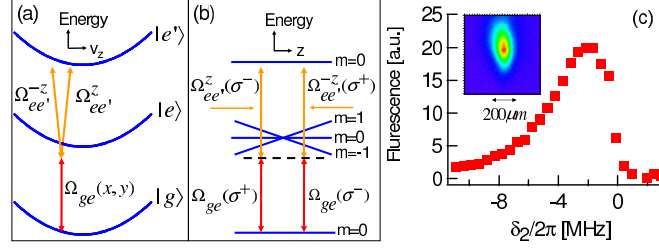


FIG. 2: (Color online) (a): Schematic illustration of the velocity damping due to the Doppler effect for 2-photon scattering. Here  $\Omega_{ee'}^{\pm z}$  represents the 6P-8S beam from the  $\pm \hat{z}$  direction. (b): Schematic illustration of the trapping force along  $z$  due to the Zeeman shift ( $z$  quantization axis) of intermediate resonance in the 2-photon scattering in a linearly changing magnetic field. Only the excitation pathway enhanced by the Zeeman shift is shown. (c): Peak fluorescence of the two-color MOT vs 2-photon detuning  $\delta_2$ . Here  $s_{ge} = 1$ ,  $s_{ee'} = 15$ . Inset gives a fluorescence image of the MOT at  $\delta_2/2\pi = -3$  MHz.

$J=0$  ground state,  $J'=1$  intermediate states and  $J''=0$  excited state. As with the cooling force, the trapping force along  $\hat{z}$  is due to the scattering of the 6P-8S light. The position dependence of this force is due to the spatially dependent Zeeman shift of the *intermediate*  $6P_{3/2}$  levels. Taking the quantization axis along  $\hat{z}$ , the 6S-6P beams in the  $x-y$  plane provide both  $\sigma$  and  $\pi$  couplings between the ground state and the intermediate states. For a magnetic field along  $+\hat{z}$ , ( $z > 0$ : right side of Fig. 2b), the intermediate detuning of the 2-photon excitation is shifted toward resonance for the excitation pathway involving a  $\sigma-$  transition to the intermediate state followed by a  $\sigma+$  transition to the excited state. As a result, the atoms at  $z > 0$  preferentially absorb the 6P-8S light propagating toward  $-\hat{z}$ , leading to a restoring force in a magnetic quadrupole field. Unlike the damping force, this restoring force has the correct sign for both positive and negative  $\delta_2$  when  $\Delta_1 < 0$ .

The above analysis is corroborated by our experimental observations. In particular, at moderate 6P-8S intensity the 2-photon detuning must be negative to achieve laser cooling along the  $z$ -direction of the trap. Surprisingly, at high intensities laser cooling and trapping behave differently. As detailed below, we found laser cooling on both the red and blue sides of the 2-photon resonance. We argue that this counter-intuitive effect is due to 3-photon and higher order scattering processes.

Our experiments capture, cool and trap atoms in a cesium vapor cell. The cooling light in the  $x-y$  plane comprises the two pairs of counter-propagating 852 nm laser beams (6S-

6P beams) with 8 mm  $1/e^2$  diameter. (See Fig. 1.) The single photon detuning  $\Delta_1/2\pi = -12.5$  MHz and the peak intensity of each beam is characterized by  $s_{ge} \equiv \frac{2\Omega_{ge}^2}{\Gamma^2}$ . The gradient of the magnetic quadruple field was 1.4 mT/cm along  $\hat{\mathbf{z}}$ . The beams along  $\hat{\mathbf{z}}$  are a pair of 795 nm laser beams (6P-8S beams), and the peak intensity of each 6P-8S beam is characterized by the parameter  $s_{ee'} \equiv \frac{2\Omega_{ee'}^2}{\gamma^2}$  [8]. We add two counter-propagating repump beams at 895 nm along  $\hat{\mathbf{x}}$ , tuned to the  $6S_{1/2} F = 3$  to  $6P_{1/2} F' = 4$  transition to keep atoms in the  $F = 4$  ground states.

With the 6P-8S beams at a moderate intensity of 20 mW/cm<sup>2</sup> ( $s_{ee'} \approx 15$ ,  $\Omega_{ee'}/2\pi \approx 4$  MHz), and guided by the 2-photon Doppler cooling picture (Fig. 2a), we set the 2-photon detuning  $\delta_2$  to small negative values, comparable to the 8S linewidth  $\gamma$ . We observe trapped atoms in the two-color MOT when the helicities of the 6P-8S beams are set to be opposite to those of the 6S-6P beams in a standard MOT (Fig. 1b, Fig. 2b). As with a standard MOT [9, 10], we find that our trap tolerates wrong helicity components in the 6P-8S beams with up to  $\approx 30\%$  in intensity. As expected, the two-color MOT is more sensitive to the repump efficiency than a standard MOT, and the counter-propagating beams need to be intensity-balanced to nullify the repump radiation pressure.

In Fig. 2c we plot the peak fluorescence of the two-color MOT vs  $\delta_2$ . At the optimal 2-photon detuning of  $\delta_2/2\pi \approx -3$  Mhz and with  $s_{ge} \approx 4$ , up to  $8 \times 10^5$  atoms at a density of  $5 \times 10^{10}/\text{cm}^3$  are accumulated in the two-color MOT from the pressure  $P \approx 10^{-5}$  Pascal ( $10^{-7}$  Torr) cesium vapor. Due to the weaker trapping and damping along  $\hat{\mathbf{z}}$ , both the spatial and velocity distributions of the atomic sample are elongated along  $\hat{\mathbf{z}}$ . The velocity spread of the atoms along  $\hat{\mathbf{x}}$  and  $\hat{\mathbf{z}}$  is characterized by effective temperatures  $T_x \approx 70$   $\mu\text{K}$  and  $T_z \approx 700$   $\mu\text{K}$ , both of which are reduced at smaller  $s_{ge}$  (see below and Fig. 4). Typical  $1/e^2$  widths of the atomic spatial distribution, fit to a Gaussian, are  $w_x \approx 300$   $\mu\text{m}$  and  $w_z \approx 600$   $\mu\text{m}$ . The number of trapped atoms is an order of magnitude smaller than that of a standard MOT under similar conditions, which is likely due to the reduced capture velocity and effective capture volume for the two-color MOT.

The 2-photon Doppler cooling picture (Fig. 2) fails dramatically at high 6P-8S beam intensities. As  $s_{ee'}$  increases, the range of  $\delta_2$  for MOT operation broadens and shifts to the red. When  $s_{ee'}$  is larger than a threshold value of  $s_{\text{th}} \approx 80$ , the two-color MOT also works at positive  $\delta_2 > \delta_{\text{th}} \approx 2\pi \times 10$  MHz (Fig. 3a). For  $s_{ee'} \approx 1.8 \times 10^3$  (not shown in Fig. 3), the two-color MOT operates for  $\delta_2$  spanning a range more than  $2\pi \times 100$  MHz ( $\gg \gamma, \Gamma$ ) on

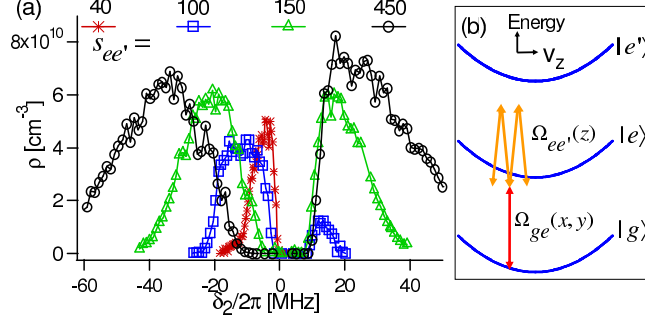


FIG. 3: (Color online) (a): Peak atom density vs two-photon detuning  $\delta_2$  for atoms in the two-color MOT at different 6P-8S beam intensities  $s_{ee'}$  and for  $s_{ge} = 4$ . (b): Schematic illustration of the velocity damping due to the Doppler effect for 3-photon scattering.

both the red and blue sides of the two-photon resonance. The maximum number of trapped atoms is similar to that achieved in the low 6P-8S beam intensity regimes, but with up to 50% increase of peak atom densities.

For high 6P-8S beam intensity and moderate 2-photon detuning, both the spatial and velocity distributions of the trapped atomic sample are more isotropic than those at low intensity. As  $s_{ee'}$  increases, the ratio  $w_z : w_x$  can reach or even go below unity at small positive  $\delta_2$ . The ratio  $T_z : T_x$  decreases and approaches unity as  $s_{ee'}$  increases, while a larger  $s_{ee'}$  is needed for the same ratio to be reached at a larger  $|\delta_2|$ . The effective temperature  $T_x$ , and remarkably, also  $T_z$ , decrease linearly with  $s_{ge}$  until the MOT stops working. For  $s_{ge} < 1$ ,  $T_z$  is well below the 125  $\mu\text{K}$  D2 Doppler limit at both large  $|\delta_2|$  as well as at small positive 2-photon detunings, as shown in Fig. 4. In addition, at large  $|\delta_2|$  the MOT becomes less sensitive to the repump efficiency and intensity balance, as in a standard MOT.

The observation of laser cooling and trapping on the blue side of the 2-photon resonance is intriguing. Equation (1) indicates that for  $\delta_2 > 0$ , the Doppler effect leads to a velocity-dependent force that becomes anti-damping. At low intensity, this precludes operation of the MOT. However, the 2-photon force picture ignores higher order scattering processes, which can be important at high intensities. These include the 3-photon process sketched in Fig. 3b in which a 2-photon absorption is followed by a stimulated emission from 8S to 6P. These multi-photon processes can lead to efficient cooling along  $\hat{z}$  in a manner similar to Doppleron cooling [11]. In the same way as for 2-photon force calculations, the 3-photon scattering force can be written as  $\mathbf{f}_z^{(3)} = 2\hbar k_{ee'} \sum_{\mathbf{i}, \mathbf{j}} R_{\mathbf{i}, \mathbf{j}}^{(3)} \hat{\mathbf{j}}$ , where, for atoms moving at velocity

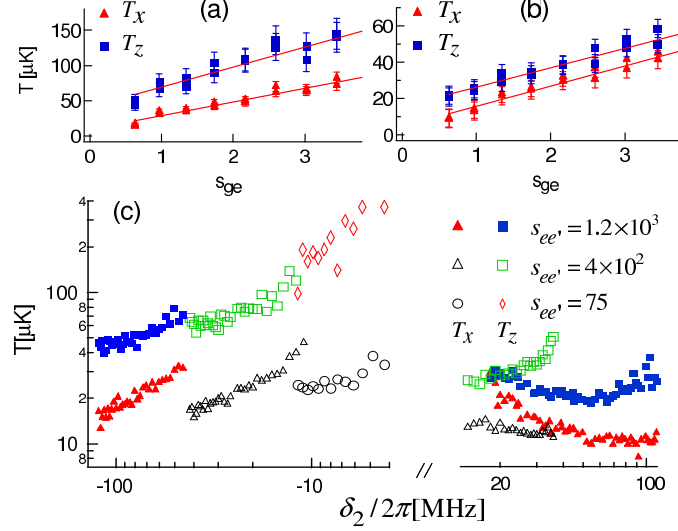


FIG. 4: (Color online) (a, b): Temperature of the atoms vs.  $s_{ge}$  for  $s_{ee'} = 1.8 \times 10^3$ , with  $\delta_2/2\pi = -143$  MHz in (a) and  $\delta_2/2\pi = 117$  MHz in (b). Notice the different temperature scales. (c): Temperature vs  $\delta_2$  for atoms in the two-color MOT at various  $s_{ee'}$  for  $s_{ge} = 0.6$ .

$\mathbf{v}$ , the 3-photon scattering rate  $R_{\hat{\mathbf{i}}, \hat{\mathbf{j}}, -\hat{\mathbf{j}}}^{(3)}$  is

$$R_{\hat{\mathbf{i}}, \hat{\mathbf{j}}, -\hat{\mathbf{j}}}^{(3)} = \frac{|\Omega_{ee'}|^2}{4|\tilde{\Delta}_1 - k_{ge}\hat{\mathbf{i}} \cdot \mathbf{v} - 2k_{ee'}\hat{\mathbf{j}} \cdot \mathbf{v}|^2} \frac{\Gamma}{\gamma} R_{\hat{\mathbf{i}}, \hat{\mathbf{j}}}^{(2)}, \quad (2)$$

with  $\tilde{\Delta}_1$  and  $R_{\hat{\mathbf{i}}, \hat{\mathbf{j}}}^{(2)}$  as in Eq. (1).

As in our treatment of Eq. (1), we Taylor-expand  $f_z^{(3)}$  near  $v_z = 0$  to find the 3-photon damping coefficient  $\alpha^{(3)}$ . For  $\Delta_1 < 0$  and  $\gamma^2 \ll \Gamma^2 + 4\Delta_1^2$ , we find  $\alpha^{(3)} > 0$  for either  $\delta_2 < 0$ , or  $\delta_2 > -\Delta_1/2$ . We note that  $\alpha^{(3)}$  involves only the 3-photon process and ignores 2-photon processes, light shifts and higher order processes. The 3-photon cooling effect at  $\delta_2 > 0$  can be understood qualitatively from the diagram in Fig. 3b: At large  $|\delta_2|$ , the Doppler sensitivity along  $\hat{\mathbf{z}}$  of the 6P-8S-6P Raman process becomes independent of  $\delta_2$ , but remains dependent on  $\Delta_1$ . The fact that  $\alpha^{(3)}$  is positive is determined by the negative single-photon detuning  $\Delta_1$ . In addition, the decreased 8S population at large  $|\delta_2|$  reduces the two-color contribution to unwanted optical pumping into the  $F = 3$  ground states, which helps explain the decreased sensitivity on repump light.

There are at least two possible explanations for the sub-6P<sub>3/2</sub>-Doppler temperatures observed along  $\hat{\mathbf{z}}$  over the wide range of 2-photon detunings in Fig. 4. First, as with sub-Doppler cooling in standard optical molasses [12], there is an interplay between spatially dependent light shifts and optical pumping among the 6S Zeeman sublevels, leading directly

to sub-Doppler cooling for atoms moving along  $\hat{\mathbf{z}}$ . This mechanism may be non-intuitive since the 852 nm light, which is the only light field that interacts with the 6S atoms, has no polarization gradient along  $\hat{\mathbf{z}}$ . However, a  $z$ -dependent ground state spin polarization can be induced by multi-photon optical pumping processes: the 6P-8S coupling dresses the  $6P_{3/2}$   $F'=5$  Zeeman sublevels, shifting and mixing those sublevels in a  $z$ -dependent way. An atom excited to a  $6P_{3/2}$   $F'=5$  dressed state is thus spin polarized, and its  $z$ -dependent polarization is partially retained after the spontaneous decay to the 6S ground states. Combined with a light shift of the ground states due to 2-color processes which is not only  $x$ -,  $y$ -dependent but also  $z$ -dependent, sub-Doppler cooling can occur along  $\hat{\mathbf{z}}$ . The inseparability of the two-color ground state light shift could also provide a second contribution to the low measured temperature along  $\hat{\mathbf{z}}$ , by mixing the standard sub-Doppler-cooled motion along  $\hat{\mathbf{x}}$ ,  $\hat{\mathbf{y}}$  with the motion along  $\hat{\mathbf{z}}$ . A quantitative analysis of this “two-color” polarization gradient cooling mechanism will appear in a future publication [13].

We have demonstrated a magneto-optical trap where cooling and trapping forces along its  $z$ -axis are provided entirely by photons associated with transitions between excited states. Up to  $8 \times 10^5$  cesium atoms are trapped in a vapor cell, and the density of the trapped atoms reaches  $8 \times 10^{10}/\text{cm}^3$  at optimal experimental parameters. Sub-Doppler cooling occurs over a wide range of positive and negative 2-photon detunings. Since we observe no density-dependent atom loss, we conclude that two-color-induced collisional loss processes are not particularly large. We believe that the number of atoms in the two-color MOT is lower than that in the standard MOT, because there is a reduced phase-space volume for capture from the room-temperature vapor. We have also observed atom cooling and trapping in a geometry complementary to the setup given by Fig. 1a, where the 852 nm beams are along  $\hat{\mathbf{z}}$ , and the 795 nm beams are along  $\hat{\mathbf{x}}$  and  $\hat{\mathbf{y}}$ , although this geometry traps even fewer atoms.

The two-color cooling and trapping demonstrated here may have practical applications. For instance, a high-numerical-aperture objective can be installed to collect 852 nm fluorescence along  $\hat{\mathbf{z}}$  in our setup, a direction along which the scattering of 6S-6P beams from the nearby optics is minimized; the 6P-8S beams at 795 nm wavelength can be easily filtered out. This would enable high-efficiency, near-background-free detection of trapped atoms. This or similar MOT arrangements may also allow completely background-free detection of fluorescence from atomic transitions driven by no laser beam. As another example, replacing regular cooling lasers with excited-state coupling lasers can be technically advantageous for



laser cooling of certain atomic species. For example, for atomic hydrogen or anti-hydrogen, the Lyman- $\alpha$  cooling transition needs 121 nm coherent radiation, which is hard to generate and manipulate [14, 15]. Instead of setting up 3 pairs of Lyman- $\alpha$  beams that couple 1S with 2P for a regular hydrogen MOT, two pairs of the beams may be replaced by laser beams that couple 2P and 3S excited states using the more readily available 656 nm light.

## Acknowledgments

We gratefully acknowledge experimental contributions by Jennifer Sebbly-Strabley, and helpful discussions with Vincent Boyer and Bruno Laburthe-Tolra.

- 
- [1] *Laser Cooling and Trapping*, H. Metcalf and P. van der Straten (Springer-Verlag, 1999).
  - [2] W. Rooijackers, W. Hogervorst, and W. Vassen, Phys. Rev. Lett. **74**, 3348, 1995; Phys. Rev. A, **56**, 3083, 1997.
  - [3] T. Binnewies, G. Wilpers, U. Sterr, F. Riehle, J. Helmcke, T. E. Mehlstäubler, E. M. Rasel and W. Ertmer, Phys. Rev. Lett. **87**, 123002, 2001.
  - [4] E. A. Curtis, C. W. Oates, and L. Hollberg, Phys. Rev. A **64**, 031403(R), 2001.
  - [5] N. Malossi, S. Dankjaer, P. L. Hansen, L. B. Jacobsen, L. Kindt, S. Sauge, J. W. Thomsen, F. C. Cruz, M. Allegrini, E. Arimondo, Phys. Rev. A **72**, 051403(R), 2005.
  - [6] E. L. Raab, M. G. Prentiss, A. Cable, S. Chu and D. E. Pritchard, Phys. Rev. Lett. **59**, 2631, 1987.
  - [7] This is in contrast to ref. [5] where the optical force due to excited state couplings is negligible.
  - [8]  $\Omega_{ge}$  and  $\Omega_{ee'}$  are specified for  $m_F = 4 - m_{F'} = 5$  and  $m_{F'} = 5 - m_{F''} = 4$  transitions respectively. We obtain  $s_{ge}$  and  $s_{ee'}$  by comparing the intensities of the laser beams with effective saturation intensities of the relevant transitions, with  $I_0 = 1.10$  mW/cm<sup>2</sup> for  $s_{ge}$  and  $I_0 = 1.32$  mW/cm<sup>2</sup> for  $s_{ee'}$ .
  - [9] C. Monroe, W. Swann, H. Robinson and C. Wieman, Phys. Rev. Lett. **65**, 1571, 1990.
  - [10] F. Shimizu, K. Shimizu and H. Takuma, Phys. Rev. A **39**, 2758, 1989.
  - [11] J. J. Tollett, J. Chen, J. G. Story, N. W. M. Ritchie, C. C. Bradley, and R. G. Hulet, Phys. Rev. Lett. **65**, 559, 1990.

- [12] J. Dalibard and C. Cohen-Tannoudji, J. Opt. Soc. B **6**, 2023, 1989.
- [13] In preparation.
- [14] I. D. Setija, H. G. C. Werij, O. J. Luiten, M. W. Reynolds, T. W. Hijmans and J. T. M. Walraven, Phys. Rev. Lett. **70**, 2257, 1993.
- [15] K. S. E. Eikema, J. Walz and T. W. Hänsch, Phys. Rev. Lett. **86**, 5679, 2001.